Proprietary Information
Withhold from Public Disclosure Under 10 CFR 2.390
This letter is decontrolled when separated from Enclosure 1

Tennessee Valley Authority, 1101 Market Street, Chattanooga, Tennessee 37402

CNL-16-145

September 23, 2016

10 CFR 50.90

ATTN: Document Control Desk
U.S. Nuclear Regulatory Commission
Washington, D.C. 20555-0001

Browns Ferry Nuclear Plant, Units 1, 2, and 3
Renewed Facility Operating License Nos. DPR-33, DPR-52, and DPR-68
NRC Docket Nos. 50-259, 50-260, and 50-296

Subject: **Proposed Technical Specifications (TS) Change TS-505 - Request for License Amendments - Extended Power Uprate (EPU) - Supplement 30, Revised Responses to Requests for Additional Information**

References:
1. Letter from TVA to NRC, CNL-15-169, "Proposed Technical Specifications (TS) Change TS-505 - Request for License Amendments - Extended Power Uprate (EPU)," dated September 21, 2015 (ML15282A152)

2. Letter from NRC to TVA, "Browns Ferry Nuclear Plant, Units 1, 2, and 3 - Request for Additional Information Related to License Amendment Request Regarding Extended Power Uprate (CAC Nos. MF6741, MF6742, and MF6743)," dated June 3, 2016 (ML16144A643)

3. Letter from TVA to NRC, CNL-16-117, "Proposed Technical Specifications (TS) Change TS-505 - Request for License Amendments - Extended Power Uprate (EPU) - Supplement 26, Responses to Requests for Additional Information," dated July 29, 2016

4. Letter from TVA to NRC, CNL-16-127, "Proposed Technical Specifications (TS) Change TS-505 - Request for License Amendments - Extended Power Uprate (EPU) - Supplement 28, Responses to Requests for Additional Information," dated August 3, 2016

By the Reference 1 letter, Tennessee Valley Authority (TVA) submitted a license amendment request (LAR) for the Extended Power Uprate (EPU) of Browns Ferry Nuclear

Plant (BFN) Units 1, 2 and 3. The proposed LAR modifies the renewed operating licenses to increase the maximum authorized core thermal power level from the current licensed thermal power of 3458 megawatts to 3952 megawatts. The Reference 2 letter provided Nuclear Regulatory Commission (NRC) Requests for Additional Information (RAIs) related to the replacement steam dryers.

Enclosure 1 to this letter provides revisions to the responses for NRC RAIs EMCB-RAIs 25, 38, 39, and 43 provided in the Reference 3 letter. Enclosure 1 to this letter also provides a revision to the response to NRC RAI EMCB-RAI 21 provided in the Reference 4 letter. These revisions to the responses to NRC RAIs EMCB-RAIs 21, 25, 38, 39, and 43 are as a result of additional reviews. GE-Hitachi Nuclear Energy Americas LLC (GEH) considers portions of the information provided in Enclosure 1 of this letter to be proprietary and, therefore, exempt from public disclosure pursuant to 10 CFR 2.390, Public inspections, exemptions, requests for withholding. An affidavit for withholding information, executed by GEH, is provided in Enclosure 3. Enclosure 2 to this letter provides a non-proprietary version of the revised responses to the RAIs provided in Enclosure 1. Therefore, on behalf of GEH, TVA requests that Enclosure 1 be withheld from public disclosure in accordance with the GEH affidavit and the provisions of 10 CFR 2.390.

TVA has reviewed the information supporting a finding of no significant hazards consideration and the environmental consideration provided to the NRC in the Reference 1 letter. The supplemental information provided in this submittal does not affect the bases for concluding that the proposed license amendment does not involve a significant hazards consideration. In addition, the supplemental information in this submittal does not affect the bases for concluding that neither an environmental impact statement nor an environmental assessment needs to be prepared in connection with the proposed license amendment. Additionally, in accordance with 10 CFR 50.91(b)(1), TVA is sending a copy of this letter to the Alabama State Department of Public Health.

There are no new regulatory commitments associated with this submittal. If there are any questions or if additional information is needed, please contact Edward D. Schrull at (423) 751-3850.

I declare under penalty of perjury that the foregoing is true and correct. Executed on the 23rd day of September 2016.

Respectfully,

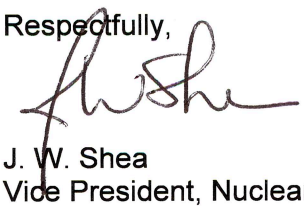

J. W. Shea
Vice President, Nuclear Licensing

Enclosures

cc: See Page 3

Enclosures:

1. Revised Responses to NRC Requests for Additional Information EMCB-RAIs 21, 25, 38, 39, and 43 (Proprietary version)

2. Revised Responses to NRC Requests for Additional Information EMCB-RAIs 21, 25, 38, 39, and 43 (Non-proprietary version)

3. General Electric Hitachi Affidavit

cc:

NRC Regional Administrator - Region II
NRC Senior Resident Inspector - Browns Ferry Nuclear Plant
State Health Officer, Alabama Department of Public Health (w/o Enclosure 1)

Withhold from Public Disclosure Under 10 CFR 2.390

ENCLOSURE 1
Revised Responses to NRC Requests for Additional Information
EMCB RAIs 21, 25, 38, 39, and 43

(Proprietary version)

ENCLOSURE 2
Revised Responses to NRC Requests for Additional Information
EMCB RAIs 21, 25, 38, 39, and 43

(Non-proprietary version)

EMCB-RAI-21

In Section 4.1.4.4.2 of NEDC-33824P (Reference 6), the [[ ]] used in estimating the [[ ]] of BFN at EPU conditions is based on [[ ]]. However, BFN and the RP have fundamental differences in the arrangement and resonance frequency of the SRVs. It is not clear why the [[ ]]. The licensee is requested to demonstrate that [[ ]]. Since the RP has additional valves other than the SRVs (e.g., ERV and TRV) which exhibited resonant response below EPU conditions, the resonant response of these other valves in the RP can be used to validate the [[ ]] which is used in BFN.

GEH Response Revision 1

Two bias terms are defined in Section 4.1.4.4.2 of NEDC-33824P. [[

]]

The second bias term addresses the difference in [[

]] (see response to EMCB-RAI-17).

The overall conservatism in the BFN SRV resonance design load is addressed in the response to EMCB-RAI-15.

Changes to NEDC-33824P Revision 0 – BFN Steam Dryer Analysis Report (SDAR)

None

EMCB-RAI-25

In Section 4.1.7.4 of NEDC-33824P (pages 4-89 to 4-101 of Reference 6), several features of the dryer acoustic loading of BFN are compared with those of other plants, including the [[ ]]. In these comparisons, the acoustic pressure characteristics are [[ ]]. This type of comparison between averages does not reflect the degree of local differences and may result in underestimating the maximum dryer stress. Since the [[ ]] is considered to be the prototype for the BFN plant, it would be appropriate to first validate this assumption by comparing the individual acoustic sources at the MSL nozzles of both plants. This comparison is needed to substantiate the [[ ]]. Therefore, the licensee is requested to compare the acoustic sources at the MSL inlets for BFN and the prototype plant at CLTP conditions. These sources can be estimated by means of MSL data based plant based load evaluation [[ ]] methodology. Please provide overlaid Power Spectral Density (PSDs) of the sources for each MSL separately.

GEH Response Revision 1

NOTE: This response is revised with an additional response appended to the end of the original response below, and as indicated with a revision bar in the right margin.

Original Response

The intent of the comparisons [[ ]] The outcome from these comparisons was [[ ]]

NEDC-33824P Section 4.1.7 presented different ways to compare the acoustic characteristics of the two plants [[ ]]

It should be noted that the key [[ ]]

NEDC-33824P presented summaries of these comparisons [[

]]

In fact, a review of [[

]] is a good representation of the similarity of the acoustic pressure loads between the [[ ]].

Note that the FIV stress analysis is performed by mapping the steam dryer acoustic nodal pressure (a total of [[ ]] nodes) onto the structural Finite Element (FE) model. The FIV analysis is performed with a very fine degree of localization, [[

]]

The main concern raised by Request for Additional Information (RAI)-25 [[

]]

The following are additional discussions and comparison plots [[

]]

Also, this RAI response includes a discussion of the comparison between [[

]]

[[ ]]

NEDC-33824P presented, in Figure 4.1-48, the BFN [[

]].

Figure 4.1-48 shows [[ ]]. However, NEDC-33824P also presented, in Figures 4.1-49 and 4.1-50, the BFN vs. [[ ]] Acoustic FRFs Pressure Distribution (3D plots) at several peak frequencies [[ ]]. A large similarity is observed in these figures, particularly the large similarity over every local area of the BFN and [[ ]] steam dryers.

More discussion is presented in NEDC-33824P Section 4.1.7.4.a.

[[ ]]

NEDC-33824P Figure 4.1-52 presented a comparison of BFN Unit 1 [[

]].

It was preferred to present the MSL pressure PSD as [[

]]

The advantage of the measured MSL comparison [[

]]

The intent of the MSL pressure comparisons [[

]]

It was indicated that it would be appropriate to [[

]]

Independently, it does not matter so much [[

]]. See the next sub-section (On-Dryer Pressure Loads) for the on-dryer pressure loads comparison and the noted degree of local similarities between the two plants.

In addition to the [[ ]], the main body of NEDC-33824P and NEDC-33824P Appendix D did include several MSL pressure comparisons per [[

]].

NEDC-33824P (Main Body):

[[

]]

NEDC-33824P Appendix D Figures 4-1 to 4-13:

[[

]]

[[ ]]

The on-dryer pressure loads comparisons are the more appropriate comparisons [[
]]

The FIV analysis is performed by mapping the steam dryer acoustic nodal pressure (a total of [[ ]] nodes) on the structural FE model. The stress analysis is directly related to the on-dryer pressure loads, [[

]].

NEDC-33824P Figure 4.1-53 presented a summary comparison of BFN [[

]].

To reflect the degree of local differences, additional comparison plots are included in the present RAI response.

[[

]]

Appendices A-1 to A-4 present additional comparison [[

]]

MSL Dead-Legs [[ ]]:

MSL Measurement:

From the MSL pressure measurements (NEDC-33824P Figure 4.1-51 and NEDC-33824P Appendix D Figures 4-1 to 4-13), [[
]].

Calculated [[ ]] Dryer Pressure Loads:

From the calculated [[ ]] pressure loads (NEDC-33824P Figure 4.1-53), and present RAI response (Appendices A-1 to A-4), [[
]]

[[

]]

Changes to NEDC-33824P Revision 0 – BFN Steam Dryer Analysis Report (SDAR):

[[

]]

[[

]]

[[

]]

GEH Additional Response to EMCB-RAI-25

Use of the [[ ]]

[[

]]

Discussion of the BWR/4 versus BFN [[ ]]

The BFN RSD pressure loads used in the RSD design analyses were reviewed [[

]]

The main cause of the difference [[

]]

With the above being stated, the predicted steam dryer loads are [[

]]

Comparisons of the [[

]]

In summary, the main cause of the differences [[

]]

In order to conservatively address the concerns [[

]]

During the investigation [[

]]

Figure 25-1

]]

[[

]]

Figure 25-1 [[ ]]

Updated ASR Based on Effect [[ ]]

A [[ ]] bias term was [[

]].

Table 25-1 [[ ]]

[[		

[[		

[[		

[[		

[[		]]

Power Ascension Test Plan Contingencies for Loss of Instrumentation

There are [[ ]] instrumentation for the lead unit:

1) [[

]]

If the [[

]]

The [[ ]] table below (Table 25-2) has been updated [[ ]].

Table 25-2 [[ ]]

[[					

[[					
					]]

[[ ]]

As discussed in the response to EMCB-RAI-39(c), [[

]]

The methods described in NEDC 33824P Appendix E are maintained [[

]]

Changes to NEDC-33824P Revision 0 – BFN Steam Dryer Analysis Report (SDAR)

1. Updated [[ ]].
2. Updated [[ ]] based on the final SDAR stress analysis results as revised by the RAI responses. [[ ]]
3. Updated [[ ]].

Appendix A for GEH Additional Response to EMCB-RAI-25 -

[[ ]]

[[

]]

Figure A-1 – [[

]]

[[

]]

Figure A-2 – [[

]]

[[

]]

Figure A-3 – [[

]]

[[

]]

Figure A-4 – [[

]]

EMCB-RAI-38

The limits in Table 5.3.1 (time) and Appendix E-1 (frequency) appear to be nonconservative compared to strains observed in other instrumented dryers.

a. Compare the simulated on-dryer strains for the BFN dryer to those measured on the benchmark BWR/4 dryer.

b. Provide cumulative strain plots for sensors [[ ]] to complement the computing root mean square (RMS) values provided in Table 5.3-1.

c. SGs 6 and 9 have very high potential strains – up to [[ ]]. SGs have a finite life, particularly at high amplitude. Provide information on which frequency(s) contribute most strongly to the strain at these gage locations. Describe the survivability (expected life or number of cycles) of the dryer SGs at these potential strain amplitudes.

d. Provide alternative procedures for RMS limits and frequency-dependent limit curves for on-dryer SGs based on new data acquired on the lead BFN dryer just prior to power ascension to CLTP. Note that since these methods would be based on data measured on the BFN dryer, [[ ]]. The current simulations of on-dryer strains may be used to demonstrate the procedure, but not used as actual limits during power ascension.

GEH Response Revision 1

NOTE: This response is revised with an additional response for part (a) appended to the end of the original response to part (a) below, and as indicated with a revision bar in the right margin. For completeness, the entire response, all parts, is provided here.

a. For comparison, the analysis scenario of the Browns Ferry Nuclear Plant (BFN) dryer Finite Element Analysis (FEA) model applied with the [[

]] was run, which is referred to as 'BFN, CR Load' later in the presented plots. In this particular analysis, [[

]]

The rationale for using the analysis [[

]]

[[

]]

Figure 38a-1. [[ ]]

[[

]]

Figure 38a-1. [[ ]]

[[

]]

Figure 38a-2. [[

]]

[[

]]

Figure 38a-3. [[

]]

[[

]]

Figure 38a-4. [[

]]

[[

]]

Figure 38a-5. [[

]]

[[

]]

Figure 38a-6. [[

]]

[[

]]

Figure 38a-7. [[

]]

[[

]]

Figure 38a-8. [[

]]

[[

]]

Figure 38a-9. [[

]]

[[

]]

Figure 38a-10. [[

]]

[[

]]

Figure 38a-11. [[

]]

[[

]]

Figure 38a-12. [[

]]

[[

]]

Figure 38a-13. [[

]]

[[

]]

Figure 38a-14. [[

]]

[[

]]

Figure 38a-15. [[

]]

[[

]]

Figure 38a-16. [[

]]

[[

]]

Figure 38a-17. [[

]]

[[

]]

Figure 38a-18. [[

]]

[[

]]

Figure 38a-19. [[

]]

GEH Additional Response to EMCB-RAI-38, Part (a)

Figures 38a-1S through 38a-18S provide the additional [[
]] comparisons between the BFN replacement dryer with the [[
]] and the BWR/4 prototype dryer with [[
]]. These two sets of [[

]]. The comparisons are provided at the [[
]]. Note in these plots, only the low frequency range (<135 Hz) is plotted, therefore the [[ ]]. Specifically, in the plots below, the legend is now detailed:

- BWR/4 Prototype: [[
]]
- BFN: [[ ]]
- Measured: [[ ]]

[[

]] as shown in NEDC-33824P R0 Table 4.1-25. [[

]] are shown in Figure 38a-1. The sensor locations are also shown in NEDC-33824P Appendix C Figures C1 to C3.

The results for the [[ ]] can be summarized as follows:

1. [[

]]

2. Design improvements have been implemented in the BFN RSD design, which are described in Section 3.2.2.2 of NEDC-33824P R0. These design improvements will [[

]]

[[

]]

Figure 38a-1S [[ ]]

[[

]]

Figure 38a-2S [[ ]]

[[

]]

Figure 38a-3S [[ ]]

[[

]]

Figure 38a-4S [[ ]]

[[

]]

Figure 38a-5S [[ ]]

[[

]]

Figure 38a-6S [[ ]]

[[

]]

Figure 38a-7S [[ ]]

[[

]]

Figure 38a-8S [[ ]]

[[

]]

Figure 38a-9S [[ ]]

[[

]]

Figure 38a-10S [[ ]]

[[

]]

Figure 38a-11S [[ ]]

[[

]]

Figure 38a-12S [[

]]

[[

]]

Figure 38a-13S [[

]]

[[

]]

Figure 38a-14S [[ ]]

[[

]]

Figure 38a-15S [[

]]

[[

]]

Figure 38a-16S [[

]]

[[

]]

Figure 38a-17S [[

]]

[[

]]

Figure 38a-18S [[

]]

b. To complement [[

]]

It is necessary to stress that [[

]]

As described in Section 5.4 of NEDC-33824P Appendix E, [[

]]

[[

]]

Figure 38b-1. [[

]]

[[

]]

Figure 38b-2. [[

]]

[[

]]

Figure 38b-3. [[

]]

[[

]]

Figure 38b-4. [[

]]

[[

]]

Figure 38b-5. [[

]]

[[

]]

Figure 38b-6. [[

]]

[[

]]

Figure 38b-7. [[

]]

[[

]]

Figure 38b-8. [[

]]

[[

]]

Figure 38b-9. [[

]]

[[

]]

Figure 38b-10. [[

]]

[[

]]

Figure 38b-11. [[

]]

[[

]]

Figure 38b-12. [[

]]

Table 38b-1. [[

]]

[[							
							]]

c. [[

]]

Table 38c-1: [[

]]

[[	
	]]

The use of the Ni-Cr-Fe fatigue Curve C (Figure 38c-1) from the American Society of Mechanical Engineers (ASME) Section III (Division 1, Appendix I, 1995) for the fatigue evaluation on the strain gage product (with the wire made of Ni-CrV) is considered conservative.

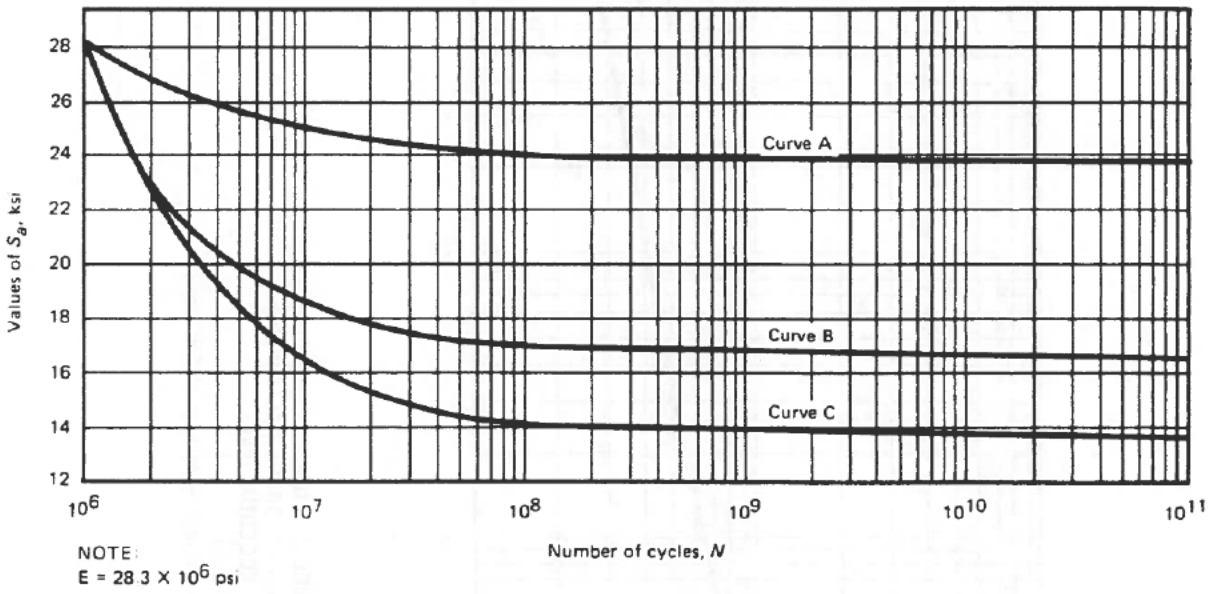

Figure 38c-1 (Figure I-9.2.2) Design Feature Curves for Austenitic Steels, Nickel-Chromium-Iron Alloy, Nickel-Iron-Chromium Alloy, and Nickel-Copper Alloy for Sa ≤ 28.2 ksi, for Temperatures Not Exceeding 800°F (For Sa>28.2 ksi, use Figure I-9.2.1)

The strain gage product specification and some supplementary test data from the manufacturer can be used to address the survivability of the strain gages. The strain gages of Model 'KHC-10-120' supplied by Kyowa Electronic Instruments Co., Ltd (Kyowa) has been and continue to be used in the BWR/4 and BWR/6 dryer EPU instrumentation process. In the product specification, the fatigue life at room temperature is identified as 4×10^5 (±1000μm/m), (i.e., 4×10^5 cycles with strain level ±1000 με (micro-strain)). The extra supplementary test data were provided by Kyowa and summarized in Table 38c-2. The test results were available in a paper (Reference 38-1) published in conjunction with the Japan Atomic Energy Research Institute (JAERI) in November 1983.

Table 38c-2: Comparison of KYOWA Fatigue Test Data with [[ ]]

	Operation Temperature	Strain Level (με)	Fatigue Life (cycles)	Strain Gage Integrity Hold/Not?
KHC Product Specification	75.2°F (24° C)	±1000	4×10^5	No information provided
KHC Test 1	932°F (500° C)	±300	$1\text{x}10^7$	Strain gage is not reported broken
KHC Test 2		**±1000**	**$2\text{x}10^6$**	**Strain gage is reported broken**
KHC Test 3		±500	$5\text{x}10^6$	Strain gage is not reported broken

[[

]] the time duration required for the power ascension test to complete, which is [[ ]].

d. The procedure for the Root Mean Square (RMS) limits and frequency-dependent limit curves for on-dryer Strain Gages (SGs) based on new data acquired on the lead BFN dryer is [[ ]]

Appendix E presented the power ascension test plan and limit curves (on-dryer and Main Steam Line (MSL) based) for the Browns Ferry Nuclear Plant (BFN) replacement steam dryers. Section 5.0 of Appendix E discussed the [[ ]] limit curves for on-dryer strain gages based on the Flow-Induced Vibration (FIV) analysis results developed from [[

]]

Lead unit power ascension process was presented in Appendix E, Figure 3.2-1. [[

]]

It is noted that for BFN dryer limit curve updates with the BFN on-dryer measurements, [[

]]

The methodology for maximum stress calculation and acceptance limit updates with on-dryer strain measurement is consistent [[

]]

[[

]]

Figure 38d-1. [[ ]]

As presented in the [[ ]] Figure 3.2-1 [[

]]

Measured Data:

[[ ]]

Predicted Data:

[[

]]

Reference

38-1. Evaluation Test of Stability for High Temperature Strain Gages (in Japanese), 共和技報, No. 309, November 1983.

Changes to NEDC-33824P Revision 0 – BFN Steam Dryer Analysis Report (SDAR):

Appendix E: Power Ascension Test Plan Limit Curves (On-Dryer & MSL Based)

[[

]]

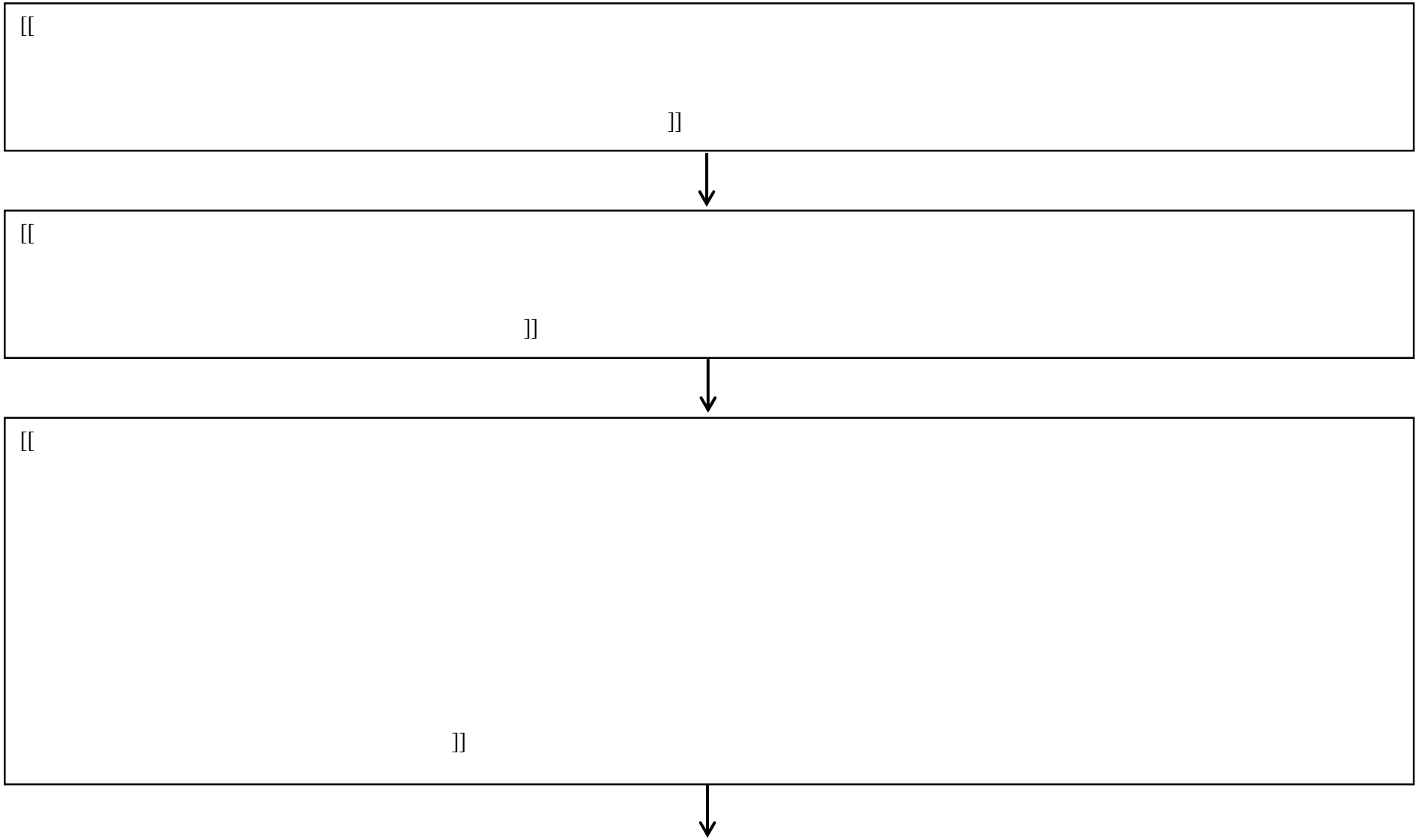

(continued on next page)

Figure 3.2-1: Browns Ferry [[ ]]

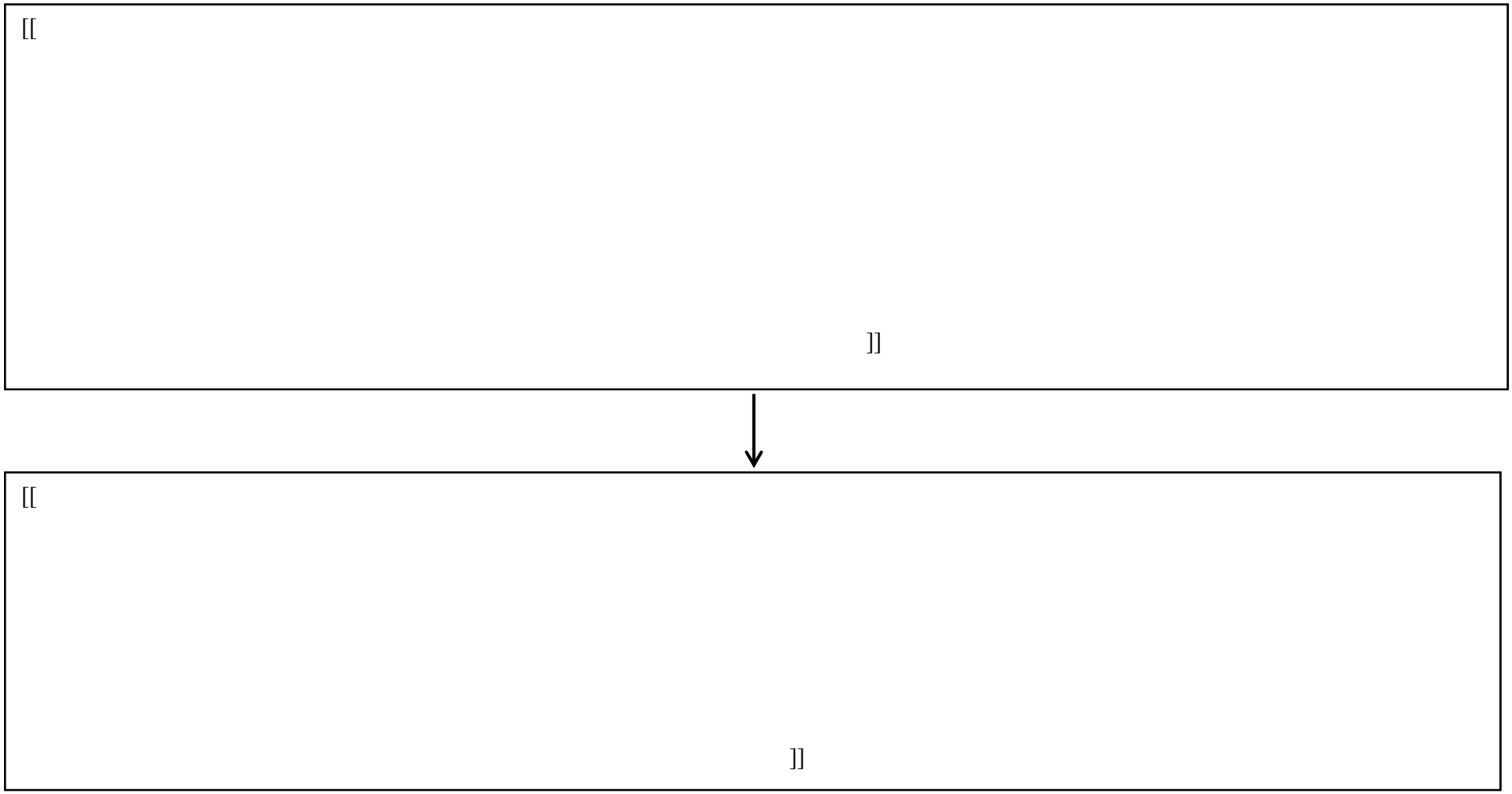

Figure 3.2-1: Browns Ferry [[ ]] **(continued)**

EMCB-RAI-39

GEH computes [[

]]. The final alternating stress ratios (ASRs) at EPU shown in Table 4.4-1 on pages 4-152 and 4-153 (Reference 6) are above 2.0, and additional details of the five most highly stressed dryer regions are provided in Section 6 of Appendix D (Reference 10) of Attachment 40 (Ref. 6). However, not enough peak stress locations were addressed in the plots provided. Provide the following additional information.

a. Table 8.1-4 of Appendix-A (p. A-88 of Reference 8) states that a [[

]]. Provide the numerical value of the [[ ]] used in the static analysis. Also, provide a justification for the magnitude of the [[ ]] value.

b. The instrument mast on BFN unit 3 RSD used for on-dryer instrumentation may influence the dryer stresses in the vicinity of the mast. Please clarify the following:

   i. Are the ASRs shown in Table 4.4-1 (pages 4-152 and 4-153 of Reference 6) based on a structural finite element model of the RSD with the instrumentation mast, without the instrumentation mast or an envelope of with and without the mast?

   ii. If the ASRs in Table 4.4-1 are based on a dryer model without the mast, provide ASRs for a model that includes the mast.

c. Based on Section 5.1 (page 5-1), and Section 4.1 (p. A-16) of Appendix-A (Reference 8) it appears that the ASRs shown in Table 4.4-1 are [[

]]. This issue is being discussed in the ASME Code committees, and has not been resolved. Therefore, provide adjusted Table 4.4-1 ASRs applying the [[

]]

d. Provide spectra and stress accumulation plots for the five most highly stressed upper dryer and for the five most highly stressed lower dryer locations. Highlight the relative contributions to total stress of the [[ ]], the SRV resonance peak(s), and the VPF peak.

GEH Response Revision 1

NOTE: This response is revised for part (c) only, as indicated with a revision bar in the right margin. For completeness, the entire response, all parts, is provided here.

a. The acoustic load on the face of the steam dryer hood during a Main Steam Line Break (MSLB) event consists of [[

]]

Figure 39-1 shows an example of the typical [[ ]] time histories for several points on the dryer hood. The [[ ]] at each location on the dryer hood can be obtained from the corresponding [[ ]] time history as shown in Figure 39-1. The acoustic loads applied on the steam dryer outer hood for the MSLB are obtained by applying the [[ ]]. To account for the dynamic effect from the MSLB transient event [[ ]]. This factor is defined [[ ]]. Because deflection, spring forces, and stresses in the linear elastic structure analysis are all proportional, the [[ ]]. In Reference 39-1 the responses for one-degree elastic systems (un-damped) subjected to symmetrical triangular load pulse are calculated. Figure 39-2 (Figure 2.6(c) in Reference 39-1) shows the typical responses for this type of forcing function which start at zero and reach a maximum F1 at one-half the total force duration t_d, with T as the natural period of the system. The maximum response as a function of t_d/T is given by Figure 39-3 (Figure 2.8(a) in Reference 39-1). [[ ]] As shown in Figure 39-1, the time histories of MSLB acoustic loads [[

]]

[[

]]

Figure 39-1. Typical Local Normalized Pressure vs Time and Peak Normalized Pressure Loads on the Hood

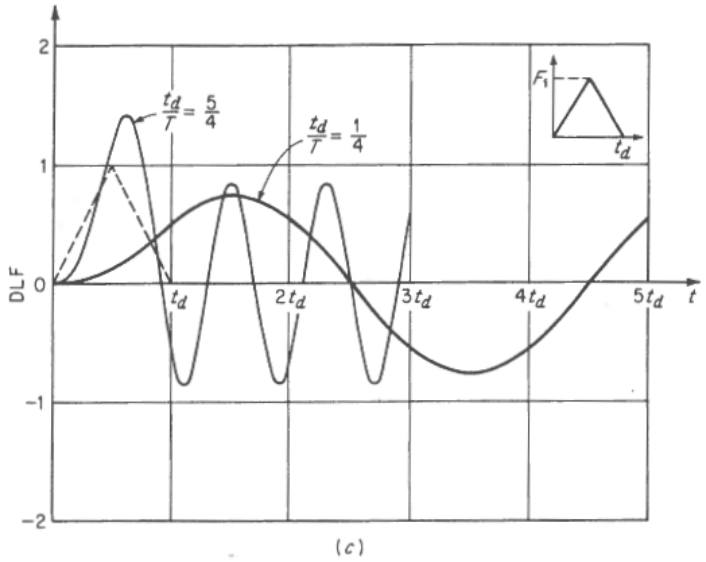

Figure 39-2. Typical Responses of One-Degree Elastic Systems (Un-damped) Subjected to Symmetrical Triangular Load Pulse (T is the natural period of the system)

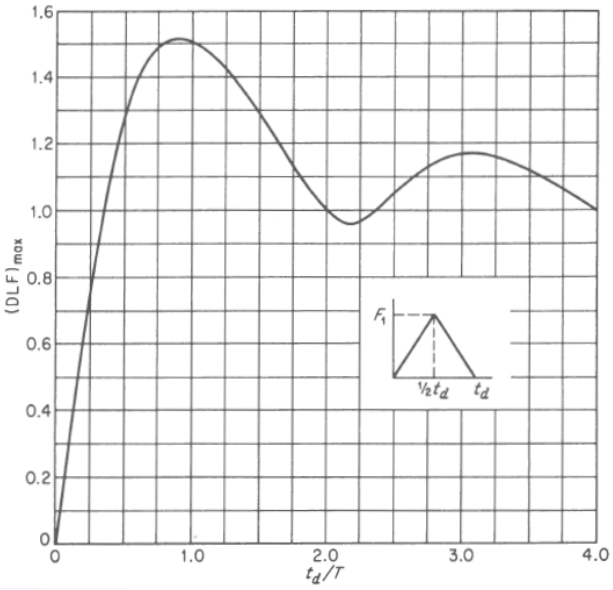

Figure 39-3. Maximum Response of One-Degree Elastic Systems (Un-damped) Subjected to Symmetrical Triangular Load Pulse (T is the natural period of the system)

b. [[

]]

Although the dryer Finite Element Model (FEM) used to generate Flow-Induced Vibration (FIV) ASR values [[

]]

To evaluate the global impact of the instrumentation mast [[
]] the RSD with and without the instrumentation mast was performed up to frequency of [[ ]], which covered the [[
]]. Resulting [[
]] by inclusion of the instrumentation mast in the model. Additionally, a selected [[ ]] was performed to evaluate the [[

]]

Figure 39-4 shows the structural finite element model of the RSD with the instrumentation mast model, [[ ]]. Table 39-1 is the [[
]] are shown in Figures 39-5, 39-6, and 39-7, which are mainly the [[ ]]. Global steam dryer [[
]]. From Figures 39-8 and 39-9, the [[
]].

[[

]]

Figure 39-4. [[ ]]

Table 39-1: [[ ]]

[[

]]

[[

]]

Figure 39-5. [[ ]]

[[

]]

Figure 39-6. [[ ]]

[[

]]

Figure 39-7. [[ ]]

[[

]]

Figure 39-8. Steam Dryer Modes at [[ ]]

[[

]]

Figure 39-9. Steam Dryer Modes at [[ ]]

To evaluate the [[ ]], the FIV stress analysis is performed to the [[

]]. The stress intensity contour plot of the component of [[ ]] is shown in Figure 39-10. The maximum stress intensity is at [[

]] is shown in Figure 39-11. The instrumentation mast is [[

]] in Figure 39-11. [[

]] When excluding the stress at these [[ ]] as shown in the close look of the [[ ]] at the bottom left of Figure 39-12, which is [[

]] as shown in Figure 39-12. [[

]] as shown in Figure 39-13, [[

]]

[[

]]

Figure 39-10. [[

]]

[[

]]

Figure 39-11. [[ ]]

[[

]]

Figure 39-12. [[

]]

[[

]]

Figure 39-13. [[

]]

In addition, all the mast structure components have been analyzed for [[

]]

c. ASRs shown in Table 4.4-1 are [[ ]]. For components with stresses calculated directly from the FEM, [[

]] from NEDC-33824P would result in some component [[

]]

Section NG-3222.4(e) of the ASME Boiler and Pressure Vessel (B&PV) Code requires correction of fatigue calculations for the Young's modulus ratio. However, as noted in Section 4.3 of NEDC-33824P the steam dryer is a non-safety related item and is classified as an Internal Structure as defined in the ASME B&PV Code, Section III. While the steam dryer is not a component governed by the ASME B&PV Code, the design complies with stress and fatigue criteria for core support structures, ASME B&PV Code Section III, Subsection NG-3000. NEDC-33824P Section 4.3 does, however, [[

]] is discussed below.

The data used to generate the fatigue curve in ASME B&PV Code, Section III, Appendix I, Table I-9.2 includes correction of the fatigue data for the effect of mean stress using the Goodman approach and strength properties at room temperature. GEH review of technical literature on the Goodman approach showed no specific limitation related to temperature. In

fact, Reference 39.3 demonstrated an application of the Goodman diagram for 600°F stainless steel data.

When the mean stress correction (MSC) is performed considering strength values at the reactor operating temperature and EC is also applied, the resulting endurance limit of the austenitic stainless steel increases significantly, see Table 39-1a.

Table39-1a Revised Fatigue Limit as a Function of Temperature for Austenitic Stainless Steel – Includes EC and MSC

Temperature (°F)	70	200	300	400	500	550	600
Revised Fatigue Limit (ksi)	13.6	15.1	15.8	15.5	15.2	15.0	14.8

Applying the revised fatigue endurance limit to NEDC-33824P Table 4.4-1 stress values would [[ ]]. Therefore, the NEDC-33824P Table 4.4-1 [[

]]. The ASR values documented in NEDC-33824P Table 4.4-1 are [[

]].

In addition to the conservatism in the design fatigue limit of 13.6 ksi when considering the [[

]], there are several additional conservatisms in the BFN replacement dryer fatigue analysis. These conservatisms were introduced in the development of the final stress adjustment terms listed in Table 4.2-7 of NEDC-33824P and are discussed below:

SRV Acoustic Resonance EPU Scale Factor: As described in the response to BFN EPU-EMCB-RAI-15, the scale model testing performed for BFN showed that the maximum measured SRV acoustic resonance pressure load at EPU was 3.5 times the SRV resonance pressure load at CLTP. [[

]].

Mesh Convergence Factor: [[

]]. The mesh convergence studies where the [[
]] was developed are described in Section 4.2.2. [[

]]

Recirculation Pump Vane Passing Frequency Loads: The recirculation pump vane passing frequency (VPF) loading is discussed in NEDC-33824P Section 4.1.5.4. There are

several conservatisms associated with the way the dryer response to the VPF loads has been addressed in the BFN RSD analysis. [[

]]

Core Flow Effect: [[

]] This core flow effect is described in Section 4.1.5.3. [[

]]

An additional conservatism was introduced into the BFN RSD stress results by the [[

]]. These concerns are described in the supplemental

response to BFN EPU-EMCB-RAI-25. To address the concerns, [[

]]. Investigation into the root causes for the [[

]]. A minor error was identified in the inputs used in the development of the [[

]]. Estimates correcting for this error [[ ]]. While this error correction may not resolve all the concerns expressed in the RAI, it does indicate that most of the difference in the dryer loads in the [[

]].

In conclusion, the fatigue acceptance criterion of 13.6 ksi used in the BFN RSD analysis is conservative when considering the temperature effects on both the Young's modulus ratio and on the maximum retained mean stress. Therefore, a separate temperature correction for the Young's modulus ratio alone is not necessary.

d. In the [[

]]

Table 39-2: [[

]]

Component Name	Time Shift Load Case	Time Interval	LF Adjusted Stress	HF Adjusted Stress	Combined Adjusted Stress	Alternating Stress Ratio
[[						
						]]

Note:
1. [[

]]

[[

]]

Figure 39-14a

[[

]]

Figure 39-14b

[[

]]

Figure 39-14c

[[

]]

Figure 39-15a

[[

]]

Figure 39-15b

[[

]]

Figure 39-15c

[[

]]

Figure 39-16a

[[

]]

Figure 39-16b

[[

]]

Figure 39-16c

[[

]]

Figure 39-17a

[[

]]

Figure 39-17b

[[

]]

Figure 39-17c

[[

]]

Figure 39-18a

[[

]]

Figure 39-18b

[[

]]

Figure 39-18c

[[

]]

Figure 39-19a

[[

]]

Figure 39-19b

[[

]]

Figure 39-19c

[[

]]

Figure 39-20a

[[

]]

Figure 39-20b

[[

]]

Figure 39-20c

[[

]]

Figure 39-21a

[[

]]

Figure 39-21b

[[

]]

Figure 39-21c

[[

]]

Figure 39-22a

[[

]]

Figure 39-22b

[[

]]

Figure 39-22c

[[

]]

Figure 39-23a

[[

]]

Figure 39-23b

[[

]]

Figure 39-23c

[[

]]

Figure 39-24a

[[

]]

Figure 39-24b

[[

]]

Figure 39-24c

References:

39-1. John M. Biggs, Introduction to Structural Dynamics, McGraw-Hill Book Companies, 1964.

39.2 An Examination of the Role of the Assumed Young's Modulus Value at the High Cycle End of ASME Code Fatigue Curve for Stainless Steels. Ranganath, Sampath and Mehta, Hardayal, S. Boston: Pressure Vessels & Piping Conference, 2015.

39.3 MJ Manjoine and RE Tome, "Proposed Design Criteria for High Cycle Fatigue of Stainless Steels," International Conference on Advances in Life Prediction Methods, ASME, 1983, pp. 51-57.

Changes to NEDC-33824P Revision 0 – BFN Steam Dryer Analysis Report (SDAR):

None

EMCB-RAI-43

Provide a quantitative justification that ANSYS shell elements used to model the steam dryer in the finite element structural analysis of the steam dryer adequately capture peak stresses.

GEH Response Revision 1

In ANSYS Version 14.0 (Reference 43-1), SHELL181 is the recommended four-node structural shell element for modeling thin to moderately-thick shell structures. The SHELL181 element formulation assumes the transverse shear is a parabolic distribution through the thickness (i.e. zero transverse shear stress at the top and bottom fibers and maximum at middle fiber). The ANSYS SHELL63 element type is a legacy element type in Version 14.0. It is formulated for analyzing relatively thin shell structures where transverse shear stiffness is negligible with respect to the in-plane stiffness. The ANSYS SHELL43 element type is also a legacy element type in Version 14.0. The SHELL43 element formulation assumes a uniform transverse shear distribution through the plate thickness and is well-suited for modeling thin to moderately thick structures. Both SHELL43 and SHELL63 element types are undocumented; however, these elements are [[ ]]. The replacement steam dryer (RSD) finite element model (FEM) [[ ]]. The reason for this choice is [[

]]

To determine the consequence of the transverse shear assumption in the ANSYS element formulation for the three element types, SHELL181, SHELL63, and SHELL43, a simplified study using the ANSYS verification manual test case VM39 (Reference 43-1) was performed. This test case uses a 10° sector of a circular plate with a center hole to study the differences between the three element types (see Figure 43-1). The plate thickness for the study is 0.25 inches and the inner (b) and outer (a) radii are 10 inches and 30 inches, respectively. For the material, the elastic modulus is 30 MSI and Poisson's ratio is 0.3. Symmetric boundary condition configurations are applied along the two radial edges with the inner diameter constrained in all six degrees of freedom. In order to test the transverse shear effect, the loading is modified as a total 4 lb. vertical force applied evenly at outer edge two nodes (Nodes 7 and 17) of the 10° sector as shown in Figure 43-1. This simplified test case configuration is similar to the [[ ]].

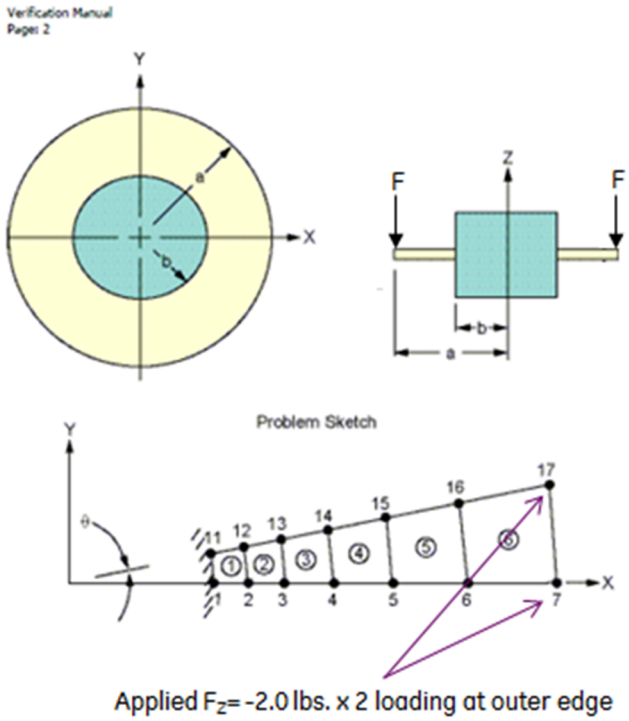

Figure 43-1 Finite Element Model Description for Test Case VM39 with Vertical Force Applied

Table 43-1 shows comparisons of the outer edge deflection and the average element component stress SX in X (~ radial) direction for the inner diameter (Element 1) and outer diameter (Element 6) elements, as well as the peak component stress SX (maximum element node stress) for the inner diameter (Element 1), using the SHELL181 (ANSYS recommended element type) results as a base reference. The comparisons show the differences to be insignificant. However, the SHELL43 results are virtually identical to the SHELL181 results for the case analyzed.

To further illustrate the ANSYS transverse shear stress assumption for the three element types, Figures 43-2 to 43-4 provide the component stress listing at each node for Element 1 for the SHELL63, SHELL181 and SHELL43 element types, respectively. The results indicate that although there is no significant difference for the dominant in-plane stresses (SX and SY); the non-zero transverse shear stresses (SXZ and SYZ) are computed for SHELL181 and SHELL43 element types and not for the SHELL63 element type. Noting that the listed output contains three sets of data for the top, bottom, and middle fibers respectively, the SHELL181 top and bottom fibers assume a zero transverse shear stress with a maximum transverse shear stress in the middle fiber, while the SHELL43 element type assumes the transverse shear stress to be distributed uniformly throughout the thickness. Therefore, to adequately model locations where the transverse shear effect cannot be neglected, the SHELL181 or SHELL43 element types are recommended.

Table 43-1 Results Obtained from SHELL63, SHELL181 and SHELL43

	SHELL181	SHELL63	SHELL43	Percent Difference (63-181)/181	Percent Difference (43-181)/181
Deflection at Outer Edge (in)	-0.05755	-0.05850	-0.05757	1.6422%	0.0201%
Average SX Stress in Element 6 (psi)	168.06	177.02	168.06	5.3263%	-0.0001%
Average SX Stress in Element 1 (psi)	2,449.00	2,424.04	2,449.01	-1.0194%	0.0002%
Peak SX Stress in Element 1 (psi)	2,515.30	2,525.40	2,515.40	0.4015%	0.0040%

```
PRINT S    ELEMENT SOLUTION PER ELEMENT

***** POST1 ELEMENT NODAL STRESS LISTING *****

 LOAD STEP=     1  SUBSTEP=     1
  TIME=    1.0000       LOAD CASE=   0
 SHELL RESULTS FOR TOP/BOTTOM ALSO MID WHERE APPROPRIATE

 THE FOLLOWING X,Y,Z VALUES ARE IN GLOBAL COORDINATES

 ELEMENT=       1        SHELL63
   NODE     SX          SY          SZ          SXY         SYZ         SXZ
      1    2525.4      749.11      0.0000     -16.783      0.0000      0.0000
      2    2373.1      1040.2      0.0000     -3.6686      0.0000      0.0000
     12    2341.5      1086.6      0.0000      233.04      0.0000      0.0000
     11    2456.2      803.78      0.0000      318.99      0.0000      0.0000
      1   -2525.4     -749.11      0.0000      16.783      0.0000      0.0000
      2   -2373.1     -1040.2      0.0000      3.6686      0.0000      0.0000
     12   -2341.5     -1086.6      0.0000     -233.04      0.0000      0.0000
     11   -2456.2     -803.78      0.0000     -318.99      0.0000      0.0000
      1    0.0000      0.0000      0.0000      0.0000      0.0000      0.0000
      2    0.0000      0.0000      0.0000      0.0000      0.0000      0.0000
     12    0.0000      0.0000      0.0000      0.0000      0.0000      0.0000
     11    0.0000      0.0000      0.0000      0.0000      0.0000      0.0000
```

Figure 43-2 Element Component Stresses (psi) for Element #1 Using SHELL63

PRINT S ELEMENT SOLUTION PER ELEMENT

***** POST1 ELEMENT NODAL STRESS LISTING *****

LOAD STEP= 1 SUBSTEP= 1
TIME= 1.0000 LOAD CASE= 0
SHELL RESULTS FOR TOP/BOTTOM ALSO MID WHERE APPROPRIATE

THE FOLLOWING X,Y,Z VALUES ARE IN GLOBAL COORDINATES

ELEMENT= 1 SHELL181

NODE	SX	SY	SZ	SXY	SYZ	SXZ
1	2406.1	731.74	0.0000	73.244	0.0000	0.0000
2	2515.3	1095.9	0.0000	62.137	0.0000	0.0000
12	2493.9	1117.5	0.0000	184.45	0.0000	0.0000
11	2380.8	757.22	0.0000	217.52	0.0000	0.0000
1	-2406.1	-731.74	0.0000	-73.244	0.0000	0.0000
2	-2515.3	-1095.9	0.0000	-62.137	0.0000	0.0000
12	-2493.9	-1117.5	0.0000	-184.45	0.0000	0.0000
11	-2380.8	-757.22	0.0000	-217.52	0.0000	0.0000
1	0.0000	0.0000	0.0000	0.0000	-1.0900	-12.459
2	0.0000	0.0000	0.0000	0.0000	-1.7399	-12.368
12	0.0000	0.0000	0.0000	0.0000	-1.7708	-12.721
11	0.0000	0.0000	0.0000	0.0000	-1.1209	-12.812

Figure 43-3 Element Component Stresses (psi) for Element #1 Using SHELL181

PRINT S ELEMENT SOLUTION PER ELEMENT

***** POST1 ELEMENT NODAL STRESS LISTING *****

LOAD STEP= 1 SUBSTEP= 1
TIME= 1.0000 LOAD CASE= 0
SHELL RESULTS FOR TOP/BOTTOM ALSO MID WHERE APPROPRIATE

THE FOLLOWING X,Y,Z VALUES ARE IN GLOBAL COORDINATES

ELEMENT= 1 SHELL43

NODE	SX	SY	SZ	SXY	SYZ	SXZ
1	2406.1	731.76	0.0000	73.245	-0.73410	-8.3908
2	2515.4	1095.9	0.0000	62.096	-0.73410	-8.3908
12	2493.8	1117.4	0.0000	184.40	-0.73410	-8.3908
11	2380.7	757.20	0.0000	217.51	-0.73410	-8.3908
1	-2406.1	-731.76	0.0000	-73.245	-0.73410	-8.3908
2	-2515.4	-1095.9	0.0000	-62.096	-0.73410	-8.3908
12	-2493.8	-1117.4	0.0000	-184.40	-0.73410	-8.3908
11	-2380.7	-757.20	0.0000	-217.51	-0.73410	-8.3908

Figure 43-4 Element Component Stresses (psi) for Element #1 Using SHELL43

During the RSD FEM development, two FIV full transient dynamic analysis test runs were performed using a [[

]]

Although SHELL181 is the ANSYS recommended element type, the VM39 case study shows that the SHELL43 element type and SHELL181 element type calculate approximately the same result. Table 43-2 presents the comparison of the [[

]] as taken from Table 4.4-1 of NEDC-33824P Revision 0. [[

]]; therefore, the results for these components are not applicable to this Request for Additional Information (RAI) response. The results show that [[

]]

The final version of the Browns Ferry Nuclear Plant (BFN) RSD FEM is primarily comprised of ANSYS [[

]]

Table 43-2

[[			

]]

In addition, a comparison of peak stresses (maximum element node stresses SX) for SHELL43, SHELL63, and SHELL181 is provided in Table 43-1. The peak stress comparison shows that the conclusion provided in Revision 0 of the response to EMCB-RAI-43 is unchanged.

It should be noted that the model used to compare SHELL181, SHELL63 and SHELL43 for the EMCB-RAI-43 response includes a stress concentration. As shown in Figure 43-1 and described in the RAI response, the test case is a 10° sector of a circular plate with a center hole. The nodes along the inner diameter of the plate are constrained in all six degrees of freedom. The 4 lb. vertical force is applied at the outer edge nodes. Similar to a cantilever beam, the higher stresses occur at the element closer to the fixed boundaries. In Table 43-1, the element component stress in X direction (SX) in Element #1 is much higher than the SX stress in Element #6, which clearly shows the stress concentration at the inner edge which is the discontinuity location. This test case configuration is similar to the base plate-to-mid support ring connection in the BFN replacement steam dryer FEM. Therefore, the results from this case study are considered to be adequate and there is no need to perform additional studies.

Reference

43-1. ANSYS Help Documentation Release 14.0 SAS IP, Inc.

Changes to NEDC-33824P Revision 0 – BFN Steam Dryer Analysis Report (SDAR)

None

ENCLOSURE 3

General Electric Hitachi Affidavit

GE-Hitachi Nuclear Energy Americas LLC

AFFIDAVIT

I, **Peter M. Yandow,** state as follows:

(1) I am Vice President, NPP/Services Licensing, Regulatory Affairs, GE-Hitachi Nuclear Energy Americas LLC (GEH), and have been delegated the function of reviewing the information described in paragraph (2) which is sought to be withheld, and have been authorized to apply for its withholding.

(2) The information sought to be withheld is contained in Enclosure 1 of GEH letter 175528-021, "GEH Revised Responses to RAIs 21, 25, 38a, 39c and 43 in Support of the Browns Ferry Steam Dryer Replacement," dated September 16, 2016. The GEH proprietary information in Enclosure 1, which is entitled "GEH Revised Responses to EMCB RAIs 25, 38a, 39c and 43 in Support of TVA Browns Ferry Replacement Steam Dryer," is identified by a dotted underline inside double square brackets. [[This sentence is an example.{3}]] Figures and large objects are identified with double square brackets before and after the object. In each case, the superscript notation {3} refers to Paragraph (3) of this affidavit, which provides the basis for the proprietary determination.

(3) In making this application for withholding of proprietary information of which it is the owner or licensee, GEH relies upon the exemption from disclosure set forth in the *Freedom of Information Act* ("FOIA"), 5 U.S.C. Sec. 552(b)(4), and the *Trade Secrets Act*, 18 U.S.C. Sec. 1905, and NRC regulations 10 CFR 9.17(a)(4), and 2.390(a)(4) for trade secrets (Exemption 4). The material for which exemption from disclosure is here sought also qualifies under the narrower definition of trade secret, within the meanings assigned to those terms for purposes of FOIA Exemption 4 in, respectively, Critical Mass Energy Project v. Nuclear Regulatory Commission, 975 F.2d 871 (D.C. Cir. 1992), and Public Citizen Health Research Group v. FDA, 704 F.2d 1280 (D.C. Cir. 1983).

(4) The information sought to be withheld is considered to be proprietary for the reasons set forth in paragraphs (4)a. and (4)b. Some examples of categories of information that fit into the definition of proprietary information are:

a. Information that discloses a process, method, or apparatus, including supporting data and analyses, where prevention of its use by GEH's competitors without license from GEH constitutes a competitive economic advantage over other companies;

b. Information that, if used by a competitor, would reduce their expenditure of resources or improve their competitive position in the design, manufacture, shipment, installation, assurance of quality, or licensing of a similar product;

c. Information that reveals aspects of past, present, or future GEH customer-funded development plans and programs, resulting in potential products to GEH;

d. Information that discloses trade secret or potentially patentable subject matter for which it may be desirable to obtain patent protection.

(5) To address 10 CFR 2.390(b)(4), the information sought to be withheld is being submitted to NRC in confidence. The information is of a sort customarily held in confidence by GEH, and is in fact so held. The information sought to be withheld has, to the best of my knowledge and belief, consistently been held in confidence by GEH, not been disclosed publicly, and not been made available in public sources. All disclosures to third parties, including any required transmittals to the NRC, have been made, or must be made, pursuant to regulatory provisions or proprietary or confidentiality agreements that provide for maintaining the information in confidence. The initial designation of this information as proprietary information, and the subsequent steps taken to prevent its unauthorized disclosure, are as set forth in the following paragraphs (6) and (7).

(6) Initial approval of proprietary treatment of a document is made by the manager of the originating component, who is the person most likely to be acquainted with the value and sensitivity of the information in relation to industry knowledge, or who is the person most likely to be subject to the terms under which it was licensed to GEH.

(7) The procedure for approval of external release of such a document typically requires review by the staff manager, project manager, principal scientist, or other equivalent authority for technical content, competitive effect, and determination of the accuracy of the proprietary designation. Disclosures outside GEH are limited to regulatory bodies, customers, and potential customers, and their agents, suppliers, and licensees, and others with a legitimate need for the information, and then only in accordance with appropriate regulatory provisions or proprietary or confidentiality agreements.

(8) The information identified in paragraph (2), above, is classified as proprietary because it contains detailed GEH design information of the methodology used in the design and analysis of the steam dryers for the GEH Boiling Water Reactor (BWR). Development of these methods, techniques, and information and their application for the design, modification, and analyses methodologies and processes was achieved at a significant cost to GEH.

The development of the evaluation processes along with the interpretation and application of the analytical results is derived from the extensive experience and information databases that constitute a major GEH asset.

(9) Public disclosure of the information sought to be withheld is likely to cause substantial harm to GEH's competitive position and foreclose or reduce the availability of profit-making opportunities. The information is part of GEH's comprehensive BWR safety and technology base, and its commercial value extends beyond the original development cost. The value of the technology base goes beyond the extensive physical database and analytical methodology and includes development of the expertise to determine and apply

the appropriate evaluation process. In addition, the technology base includes the value derived from providing analyses done with NRC-approved methods.

The research, development, engineering, analytical and NRC review costs comprise a substantial investment of time and money by GEH. The precise value of the expertise to devise an evaluation process and apply the correct analytical methodology is difficult to quantify, but it clearly is substantial. GEH's competitive advantage will be lost if its competitors are able to use the results of the GEH experience to normalize or verify their own process or if they are able to claim an equivalent understanding by demonstrating that they can arrive at the same or similar conclusions.

The value of this information to GEH would be lost if the information were disclosed to the public. Making such information available to competitors without their having been required to undertake a similar expenditure of resources would unfairly provide competitors with a windfall, and deprive GEH of the opportunity to exercise its competitive advantage to seek an adequate return on its large investment in developing and obtaining these very valuable analytical tools.

I declare under penalty of perjury that the foregoing is true and correct.

Executed on this 16th day of September 2016.

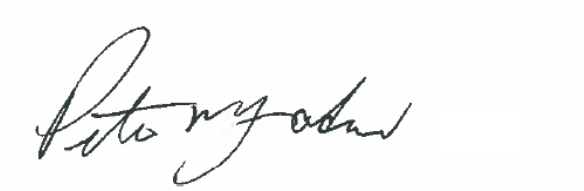

Peter M. Yandow
Vice President, NPP/Services Licensing
Regulatory Affairs
GE-Hitachi Nuclear Energy Americas LLC
3901 Castle Hayne Road
Wilmington, NC 28401
Peter.Yandow@ge.com